

---

# **Kinetic and Kinematic Responses of the RID2a, Hybrid III and Human Volunteers in Low-Speed Rear-End Collisions**

**Gunter P. Siegmund, Bradley E. Heinrichs and Jonathan M. Lawrence**  
MacInnis Engineering Associates

**Mat M.G.M. Philippens**  
TNO Automotive, Crash Safety Research Center

Reprinted From: **Stapp Car Crash Journal, Vol. 45 (November 2001)**  
(P-375)

Except for papers authored solely by one or more U.S. Government employees in the course of their employment, this journal and the materials contained herein are protected by copyright. For authorization to photocopy for internal, personal, or educational use beyond that permitted by Sections 107 or 108 of the U.S. Copyright Act, contact the Copyright Clearance Center, Inc. Operations Center, 222 Rosewood Drive, Danvers, MA 01923 USA Phone (978)750-8400 Fax (978)750-4470. Authorization does not extend to systematic or multiple reproduction, to copying for promotional purposes, to electronic storage or distribution, or to replications in any form. In all such cases, specific written permission from The Stapp Association must be obtained.

Orders and quantity reprint rates can be obtained from the SAE Customer Sales and Satisfaction Department.



**GLOBAL MOBILITY** DATABASE

*All SAE papers, standards, and selected books are abstracted and indexed in the Global Mobility Database*

No part of this publication may be reproduced in any form, in an electronic retrieval system or otherwise, without the prior written permission of the publisher.

**ISSN 0148-7191**

**Copyright © 2001 The Stapp Association**

Positions and opinions advanced in this paper are those of the author(s) and not necessarily those of SAE. The author is solely responsible for the content of the paper. A process is available by which discussions will be printed with the paper if it is published in SAE Transactions.

Persons wishing to submit papers to be considered for presentation or publication through SAE should send the manuscript or a 300 word abstract of a proposed manuscript to: Secretary, Engineering Meetings Board, SAE.

**Printed in USA**

*Stapp Car Crash Journal*, Vol. 45 (November 2001), pp.  
Copyright © 2001 The Stapp Association

## **Kinetic and Kinematic Responses of the RID2a, Hybrid III and Human Volunteers in Low-Speed Rear-End Collisions**

Gunter P. Siegmund, Bradley E. Heinrichs, Jonathan M. Lawrence  
MacInnis Engineering Associates, Richmond, BC, Canada

Mat M.G.M. Philippens  
TNO Automotive, Crash Safety Research Center, Delft, The Netherlands

---

**ABSTRACT** – An anthropomorphic test device (ATD) which accurately models the kinematic and kinetic responses of human subjects during head restraint contact in low-speed rear-end collisions is needed to evaluate present and future seat and vehicle designs. The primary goal of this study was to quantify the biofidelity of a new rear-impact ATD, the RID2a, by comparing its dynamic response to those of human subjects under identical test conditions. For this study, a RID2a and a Hybrid III ATD were each exposed to 10 low-speed rear-end collisions: five at a speed change of 4 km/h and five at a speed change of 8 km/h. Sagittal plane kinematics of the head and upper torso, head restraint contact forces, and the reaction loads and moment at the atlanto-occipital joint were determined and compared to the response of eleven male human subjects. Both ATDs produced repeatable response corridors. As observed by others, the Hybrid III did not replicate many features of the human response. Aside from the vertical response of the head and T1 in the global reference frame, the kinematic and kinetic responses of the RID2a reproduced most features of the human response. Head restraint forces observed in both the human subjects and the RID2a contained large vertical components that placed the neck in tension during head restraint contact. The results of this study indicated that the RID2a was able to model the overall kinematic and kinetic responses relevant to some recently-proposed mechanisms of whiplash injury.

**KEYWORDS** – Whiplash, Anthropomorphic test device, Human subjects, Response corridors, Head restraint, Biomechanics

---

### **INTRODUCTION**

The biomechanics of whiplash injury have been studied using human subjects, cadavers, anthropomorphic test devices (ATDs) and mathematical models – all with the goal of understanding and ultimately preventing whiplash injuries. ATDs play an important role in the design and compliance testing of automobiles and seats because, unlike cadavers and humans subject, they are repeatable and can be used over a broad range of collision severities without injurious consequences. As models of the human response to whiplash loading, however, the dynamic response of ATDs must first be validated against human responses.

The dynamic response of ATDs is a balance between biofidelity and repeatability. Some aspects of the human response, such as the overall kinematics and kinetics, must be captured by the ATD response, whereas other aspects of the human response, such as large within-subject and between-subjects variability, must not. Ultimately, the most important requirement

for an ATD is a response graded to collision, vehicle and seat variables related to the injury under investigation. This is a formidable challenge in the design of ATDs for whiplash testing because the etiology of whiplash injury and the factors that affect the potential for whiplash injury remain poorly understood. As a result, validation studies of ATDs designed for whiplash testing have focused on replicating subtle aspects of the dynamic response observed in human subjects exposed to rear-end impacts.

Numerous researchers have documented differences in the head and torso kinematics between human subjects and ATDs, like the Hybrid III, designed for high speed crash testing (Severy et al., 1955; Mertz and Patrick, 1967; Scott et al., 1993; Geigl et al., 1995; Davidsson et al., 1999a, 1999b; Gotou et al., 1999; Cappon et al., 2000). Specially designed rear-impact dummy (RID) necks were developed to address these differences (Svensson and Lövsund, 1992; Thunnissen et al., 1996), however, these solutions underestimated the contribution of the

upper torso in generating a human-like head and neck response during whiplash loading. Subsequent development has yielded two new rear-impact ATDs that attempt to reproduce the T1 kinematics by introducing articulations in the thoracic spine: the BioRID (Davidsson et al., 2000) and the RID2 (Cappon et al., 2000). A prototype version of the latter ATD, the RID2a, was evaluated in the current study.

Before being used to develop new head restraint systems, the kinematic and kinetic responses of whiplash ATDs need to be validated under conditions of head restraint contact. A number of researchers have compared the kinematic responses of human subjects and whiplash ATDs during head restraint contact (Geigl et al., 1995; Davidsson et al., 1999b; Cappon et al., 2000), however, comparisons of the kinetic responses have only been conducted in the absence of head restraint contact (Davidsson, 1999a).

The goal of this study was to compare the kinematic and kinetic responses of two ATDs and human subjects exposed to low-speed rear-end collisions in which head restraint contact occurred. In addition to comparing the linear and angular kinematic responses of the head and neck, the loads applied to the head restraint and the reaction loads and moment at the atlanto-occipital joint were compared. The results of this study help establish the kinematic and kinetic biofidelity of the ATDs, and provide some insight into how head restraint design can affect neck loading during whiplash exposures.

## METHODS

The human subject data used in this study were drawn from previous human subject experiments (Siegmund et al., 1997). The same vehicle, seat and collision severities used for the human subjects were re-used for the ATD experiments (Figures 1a-c). Only relevant details regarding the human subject experiments have been included in the present paper.

### Human Subjects

Data from eleven of the 21 male subjects previously tested were used for this comparison (Siegmund et al., 1997). These subjects were selected because their height ( $174.9 \pm 1.7$  cm; range 173 - 178 cm) was within 3 cm of a 50<sup>th</sup> percentile male ( $174.7$  cm; Diffrient et al., 1974). The mass of these subjects ( $73.5 \pm 8.6$  kg; range 63 - 87 kg) varied between the 10<sup>th</sup> and 75<sup>th</sup> percentile mass for males of the 50<sup>th</sup> percentile height (Najjar and Rowland, 1987).

### Anthropomorphic Test Devices

Two ATDs were used: a Hybrid III 50<sup>th</sup>-percentile male ATD (First Technology Safety Systems,

Plymouth, MI) and a prototype of the new rear-impact ATD, RID2a (TNO, Delft, The Netherlands). A detailed description of the modifications which comprise the RID2a can be found elsewhere (Cappon et al., 2000). Briefly, the RID2a consisted of a new neck, a THOR ribcage, new upper and lower spine components joined by a flexible T5-T8 element, and a modified Hybrid III pelvis. The same Hybrid III head and limbs were used for both ATDs. The mass of the Hybrid III ATD was 78 kg and the mass of the RID2a was 81 kg. The Hybrid III was dressed in two layers of lycra to minimize friction between the ATD and seat back (Davidsson, 1999). The RID2a was dressed in the neoprene suit supplied by the manufacturer.

### Instrumentation

For the human subjects, head acceleration was measured using a nine accelerometer array (Kistler 8302B20S1;  $\pm 20g$ , Amherst, NY) arranged in a 3-2-2-2 configuration (Padgaokar et al., 1975) and secured tightly to the forehead with adhesive and two straps. Torso acceleration was measured using a tri-axial accelerometer (Summit 34103A;  $\pm 7.5g$ , Akron, OH) and an angular rate sensor (DynaCube, ATA-Sensors, Albuquerque, NM) applied with adhesive and straps to the chest immediately below the manubrium. Head restraint loads and moments were determined using strain gauges applied to modified head restraint mounting brackets to create a custom 6-axis load cell (Lawrence et al., 1997).

Both ATDs used the same instrumentation. An array of five linear accelerometers (ROTAC-2D5/200, TNO, The Netherlands) was mounted inside the head to measure sagittal plane linear accelerations ( $a_x$ ,  $a_z$ ) and angular accelerations ( $\alpha_y$ ). A six-axis, low-capacity upper neck load cell (IF-207, First Technology Safety Systems, Plymouth, MI) was installed, however, only the sagittal plane responses ( $R_x$ ,  $R_z$ , and  $M_y$ ) were recorded. A six-axis load cell (2544A, R.A. Denton, Rochester Hills, MI) was incorporated into the skull cap to measure loads and moments during head restraint contact. Linear accelerations at T1 and in the pelvis were measured using pairs of orthogonally-mounted uni-axial accelerometers (7264B-2000, Endevco, San Juan Capistrano, CA). Angular kinematics at T1 were measured using a tri-axial angular rate sensor (DynaCube, ATA Sensors, Albuquerque, NM) on the Hybrid III and a uni-axial angular rate sensor (ARS-04E, ATA Sensors, Albuquerque, NM) on the RID2a. The same externally-mounted 3-2-2-2 accelerometer array and mounting apparatus used for the human subjects were also fastened externally to the head of both ATDs to provide a direct comparison between the different sensors used to measure linear and angular head acceleration in the humans and ATDs.

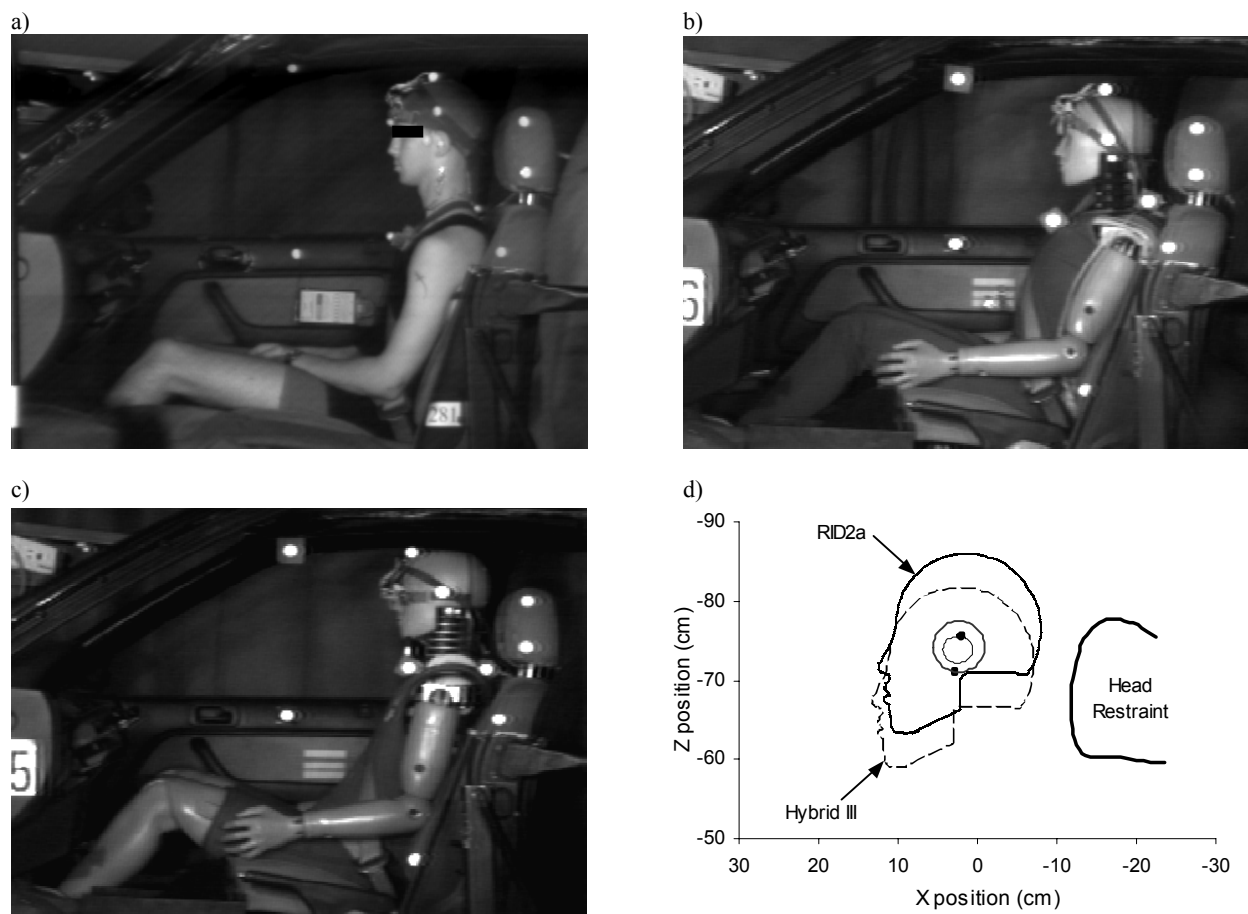


Figure 1. View of an exemplar human subject (a), Hybrid III (b), and RID2a (c) seated in the vehicle immediately before impact. Schematic (d) depicts the mean head position of the Hybrid III (dashed line) and RID2a (solid line) relative to the head restraint. The range of head centre-of-mass positions for the human subjects is outlined by the thick outer ellipse; 1 SD from the mean position is outlined by the thin inner ellipse. Solid points depict the head centre of mass for the Hybrid III (lower) and RID2a (upper). The origin ( $x = 0, z = 0$ ) for the schematic is located at the seat hinge.

The acceleration of the target vehicle during the collision was measured using a tri-axial accelerometer (34103A;  $\pm 7.5g$ , Summit Instruments, Akron, OH) mounted to the transmission tunnel near the centre of mass of the vehicle. Speed and speed change were measured with a 5<sup>th</sup> wheel (MacInnis Engineering, Richmond, BC) attached to each of the vehicles used in this study. Bumper contact was detected with ribbon switches (121BP, Nortel TapeSwitch, Scarborough, ON) applied to the rear bumper of the target vehicle. Head restraint contact was detected with a force sensitive resistor (FSR#406, Interlink Electronics, Camarillo, CA) applied to the front of the head restraint in the region of initial contact.

Transducer and contact switch data were acquired for 2 seconds at 10 kHz using 12-bit, simultaneous-sample-and-hold Win30 DAQ cards (United Electronics Incorporated, Watertown, MA) driven by a single external clock. Each data channel conformed

to SAE J211, Channel Class 1000 (SAE, 1989). Fifth wheel data were acquired at 128 Hz for 1 s before and 4 s after impact, and acquisition was triggered by the bumper contact switch.

Digital video of the sagittal plane motion was captured using an OmniSpeed HS motion capture system (Speed Vision Technologies, Solana Beach, CA) and high-speed camera (JCLabs 250; 512 x 216 lines resolution, Mountain View, CA). Video data were recorded at 250 frames per second using a shutter speed of 1/1000 s. Reflective targets were applied to the vehicle, seat and subjects (Figures 1a-c). The video data were digitized using OmniSpeed AutoTracker software with a combined experimental setup and video system accuracy of  $\pm 2$  mm at the vertical plane containing the seat centerline. The position of the video targets were measured relative to anatomical landmarks on the human subjects and relative to the origins of the head and T1 coordinate systems on the ATDs using a three-dimensional

digitizer (FaroArm B08-02, Lake Mary, FL) with single-point accuracy of  $\pm 0.30$  mm. LEDs indicating bumper and head restraint contact were placed in the camera's field of view for synchronization.

### Test Procedures

The human subjects and ATDs were seated in the front passenger seat of a 1990 Honda Accord LX 4-door sedan (Figures 1a-c). The rear of the Honda was struck by the front of a 1981 Volvo 240DL station wagon for the human subject tests and the front of a 1984 Volvo 244DL sedan for the ATD tests. The Volvos' impact speeds were selected to produce speed changes of about 4 and 8 km/h on the Honda. The Honda's passenger seat was locked in the full rear position and the initial seat back angle was set to about 27 degrees from the vertical for all tests. The head restraint was locked in the full-up position. The human subjects and ATDs were restrained by a lap and shoulder seat belt.

Human subjects were instructed to sit normally in the seat, face forward with their head level, place their hands on their lap, and relax prior to impact. Electromyographic activity in the sternocleidomastoid and cervical paraspinal muscles was monitored bilaterally using surface electrodes for at least one-minute before impact to ensure quiescent neck muscle activity. Subjects knew an impact was imminent, but could not predict its exact timing. The ATDs were placed in the seat so that their seated posture was similar to that of the human subjects. The horizontal distance between the back of the ATDs' head and the front of the head restraint was set to 4.5 cm – similar to the mean backset observed in the self-selected head position of the human subjects ( $4.6 \pm 1.7$  cm; range 1.6 – 7.8 cm). The initial position of the ATDs prior to each test was digitized using the FaroArm to quantify repeatability. Tilt sensors installed in the RID2a were also recorded prior to each test to ensure a repeatable initial position.

Each human subject underwent two tests: one at a speed change of 4 km/h and the other at a speed change of 8 km/h. To minimize the effect of habituation (Siegmund, 2001), no practice or demonstration trials were given and the two tests were separated by at least one week. Each ATD underwent ten tests: five at a speed change of 4 km/h and five at a speed change of 8 km/h. The two ATDs were tested sequentially; first the Hybrid III and then the RID2a. Within each block of an ATD's ten tests, the order of the different collision severities was randomized.

### Data Reduction

Accelerations were determined from the transducer

data and displacements were determined from the high speed video data. Kinematic data and head restraint load data were resolved into a global reference frame with the x-axis horizontal and positive forward, the y-axis horizontal and positive to the right, and the z-axis vertical and positive downward. In this reference frame, extension motions were positive and flexion motions were negative. Kinetic data at the atlanto-occipital (AO) joint were resolved to the head reference frame, in which the z-axis was positive in the inferior direction. The instantaneous orientation of the head reference frame relative to the global reference frame was determined from the high-speed video. All accelerations were corrected throughout the motion for the DC offset introduced by gravity.

For the human subjects, head accelerations were resolved to the centre of mass of the head, estimated using the same data and methods used to design the ATD head (Hubbard and McLeod, 1974). T1 accelerations were resolved to the centre of rotation of the base of the neck, estimated to be at the midpoint between the C7 spinous process and the manubrium (Queisser et al., 1994). In the ATDs, head accelerations were measured at the head's centre of mass and T1 accelerations were resolved to a point at the centre of the neck mounting location. The moment measured by the upper neck load cell in the ATDs was corrected to the AO pin. Data from the upper neck load cell were reported with both the initial head weight and the initial moment generated by the horizontal offset between the head centre of mass and the AO joint location included.

The forces and moments at the AO joint were measured directly in the ATDs by the upper neck load cell. In the human subjects, rigid body kinematics were used to compute the reactions forces and moments at the AO joint. The location of the AO joint for each subject was determined from magnetic resonance (MR) images taken as part of the pre-screening procedure. The offset ( $h$ ) of the instantaneous line of action of the head restraint force was first determined by dividing the head restraint moment ( $M_{hr}$ ) by the resultant force in the xz-plane ( $F_{hr}$ ) (Figure 2). The head restraint force was then resolved into the global reference frame by correcting for the angular displacement of the seat back, and was reported as the force applied to the head restraint by the head.

Video targets on the head and head restraint were used to transfer the instantaneous line of action of the head restraint force into the instantaneous head reference frame. The reaction forces ( $R_x$  and  $R_z$ ) and moment ( $M_y$ ) computed at the AO joint were resolved into the head reference frame (not the global reference frame) and were reported as the loads

applied to the head by the neck. The head restraint force was only included in the computation of AO joint kinetics during the interval of head restraint contact. The onset of head restraint contact was determined from the force-sensitive resistor applied to the front of the head restraint. Termination of head restraint was assumed to occur when the magnitude of the resultant head restraint force returned to its level at the onset of contact. The magnitudes of the head restraint forces and moments at head restraint contact were assumed to equal the inertial response of the head restraint and these offsets were subtracted before the rigid body computation.

**Analysis**

Two analyses were performed with the current data. The first analysis consisted of comparisons between the different transducers used for the human subjects and ATDs, and was performed to confirm that the different systems could be reliably compared. These comparisons were performed by placing both sets of transducers on the ATDs and then directly comparing the data recorded within a single test. Three sets of response variables were compared. First, head acceleration data obtained from the externally-mounted 3-2-2-2 accelerometer array were compared to data obtained from the internally-mounted ROTAC transducers. Second, loads measured by the strain-gauged head restraint were compared to loads measured by the skull cap transducer. And finally, the AO joint loads computed by inverse dynamics using accelerations measured by the 3-2-2-2 array and loads measured at the head restraint were compared to the AO joint loads measured directly by the upper neck load cell.

The second analysis consisted of comparisons between the human data and ATD data, and was performed to examine how well the ATDs reproduced the responses observed in the human subjects. To eliminate the effect of small systematic differences between the external transducers used for the humans and the internal transducers used for the ATDs, comparisons between the human subjects and ATDs were made, where possible, using the external transducers. More specifically, the head kinematics and AO joint kinetics computed from the 3-2-2-2 array and head restraint loads were used in the comparison. Corridors for the human subject data were derived using one standard deviation either side of the mean response.

**RESULTS**

The acceleration and speed change of the collisions were similar for the human subjects and ATDs (Table 1, Figure 3). The horizontal and vertical positions of the ATDs' head and H-point were well reproduced

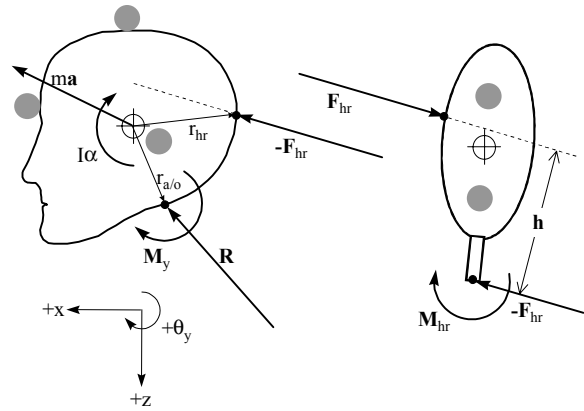


Figure 2. Free body diagrams of the head and head restraint during head restraint contact. Head and head restraint shown separated to highlight the head restraint force ( $F_{hr}$ ) and the instantaneous line of action of this force. Shaded circles indicate video targets used to determine the instantaneous orientation of the head with respect to the head restraint.

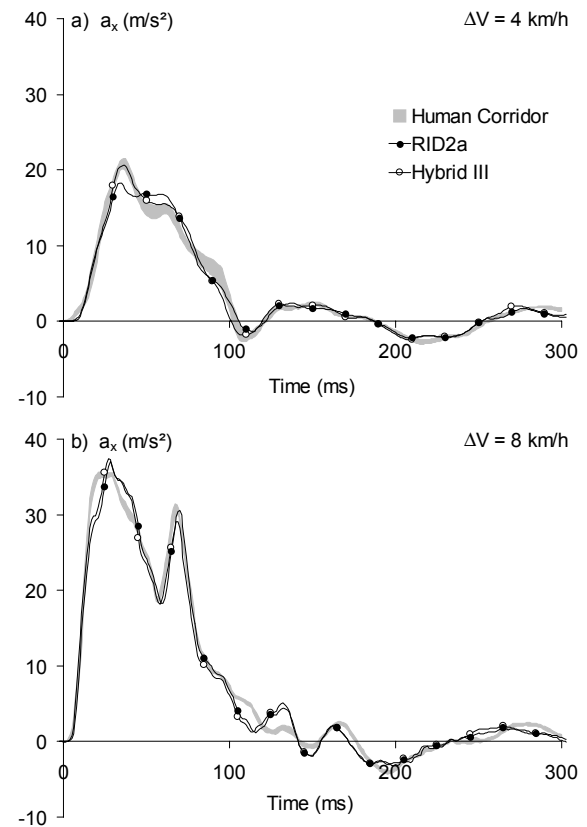


Figure 3. Horizontal acceleration ( $a_x$ ) of the target vehicle for the 4 km/h (a) and 8 km/h (b) collisions. The shaded area represents the corridor ( $\pm 1$  standard deviation) from the human subject tests. The lines represent mean data from the Hybrid III (O) and RID2a (●) tests.

Table 1. Mean (SD) of the speed change ( $\Delta V$ ) and peak acceleration ( $a_p$ ) for collisions at the 4 and 8 km/h levels.

	4 km/h level		8 km/h level	
	$\Delta V$ (km/h)	$a_p$ (m/s <sup>2</sup> )	$\Delta V$ (km/h)	$a_p$ (m/s <sup>2</sup> )
Humans	3.92 (0.11)	21.0 (0.7)	8.12 (0.10)	35.5 (0.2)
Hybrid III	4.00 (0.02)	20.7 (1.4)	7.87 (0.04)	37.4 (0.2)
RID2a	3.99 (0.05)	18.6 (0.3)	7.87 (0.03)	37.2 (0.2)

Table 2. Mean (SD) of the initial position of the head centre of mass (CoM) and H point, and the initial head restraint backset for the human subjects, Hybrid III and RID2a. The x and z coordinates are given in the global reference frame relative to an origin at the seat back hinge.

Parameter		Humans	Hybrid III	RID2a
Head CoM (cm)	x	2.5 (1.8)	2.9 (0.2)	2.1 (0.3)
	z	-73.8 (1.7)	-71.1 (0.3)	-75.5 (0.3)
H point (cm)*	x	20.7 (2.4)	11.0 (0.4)	15.8 (0.3)
	z	9.9 (1.3)	-11.5 (0.4)	-12.0 (0.2)
Backset (cm)		4.6 (1.7)	4.7 (0.3)	4.3 (0.2)

\* greater trochanter on the human subjects

between trials (Table 2). The head restraint backset of the ATDs matched the mean backset observed in the human subjects (mean 4.6 cm, range 1.6 to 7.8 cm) and indicated that the mean initial horizontal position of the head was similar for the humans and ATDs (Table 2). The initial vertical position of each ATD's head was governed by the ATD's seated height. Once seated in the vehicle, the initial vertical head position of the RID2a was 1.7 cm above the mean human head position, whereas the initial vertical head position of the Hybrid III was 2.7 cm below the mean human head position (Figure 1d). The initial vertical head positions of both ATDs were within the range of the human head positions, which varied from 3.6 cm above to 2.9 cm below the mean position.

None of the human subjects exhibited muscle activity prior to the collision. During the 4 km/h speed change, reflex activation of the neck musculature in the human subjects occurred  $94 \pm 8$  ms after bumper contact and head restraint contact occurred  $128 \pm 14$  ms after bumper contact. During the 8 km/h speed change, reflex neck muscle activation occurred  $84 \pm 6$  ms after bumper contact and head restraint contact occurred  $100 \pm 11$  ms after bumper contact. For the Hybrid III, head restraint contact did not occur at the 4 km/h level, but occurred  $117 \pm 2$  ms after bumper contact at the 8 km/h level. For the RID2a, head restraint contact occurred at  $127 \pm 3$  ms and  $100 \pm 2$  ms after bumper contact during the 4 and 8 km/h speed changes respectively.

## Transducer comparisons

The linear and angular accelerations measured by the externally-mounted 3-2-2-2 accelerometer array were similar to those measured by the internally-mounted ROTAC sensors (Figures 4a-c). The 4 ms lag between the ROTAC and 3-2-2-2 accelerometer arrays likely stemmed from compliance in the vinyl skin of the ATD's head. Head restraint loads were similar to those measured by the skull cap load cell, though of slightly smaller magnitude (Figures 4d-f). Despite these differences, the AO joint loads and moment computed using data from the 3-2-2-2 array and the head restraint were similar to those measured at the AO joint using the upper neck load cell (Figures 4g-i).

## Comparison between human subjects and ATDs

The kinematic and kinetic responses of the human subjects and both ATDs are summarized in Figures 5 through 8. Sample video sequences have also been included in Appendix A. Figures 5 through 8 were arranged so that the linear x-axis response variables are in the left column, the linear z-axis response variables are in the middle column, and the angular y-axis response variables are in the right column. For all variables, the ATD responses were repeatable (see the coefficients of variation in Table 3), and therefore only the mean responses of both ATDs were shown relative to the human subject corridors.

Both ATDs produced horizontal T1 accelerations that were similar to the human subjects (Figures 5a and 7a). The horizontal head acceleration of the Hybrid III started too early at both the 4 and 8 km/h levels, whereas the RID2a remained largely within the human subject corridors (Figures 5g and 7g). At the 4 km/h level, the head of the Hybrid III did not make head restraint contact, which resulted in a peak horizontal head acceleration for the Hybrid III that was below that observed in the human subjects (Figure 5g). The horizontal acceleration and displacement of the head relative to T1 in both ATDs was similar to the human subjects, particularly at the 8 km/h level (Figures 5m,p and 7m,p).

The good agreement observed in the horizontal components of the linear kinematics was not present in the vertical components. In the global reference frame, the head and T1 of both ATDs accelerated downward immediately after impact, whereas the head and T1 of the human subjects accelerated upward (Figures 5b,h and 7b,h). Despite these opposing absolute kinematics, the vertical acceleration of the head relative to T1 at the 8 km/h level in the RID2a was similar to the human subjects, but temporally advanced (Figure 7n).

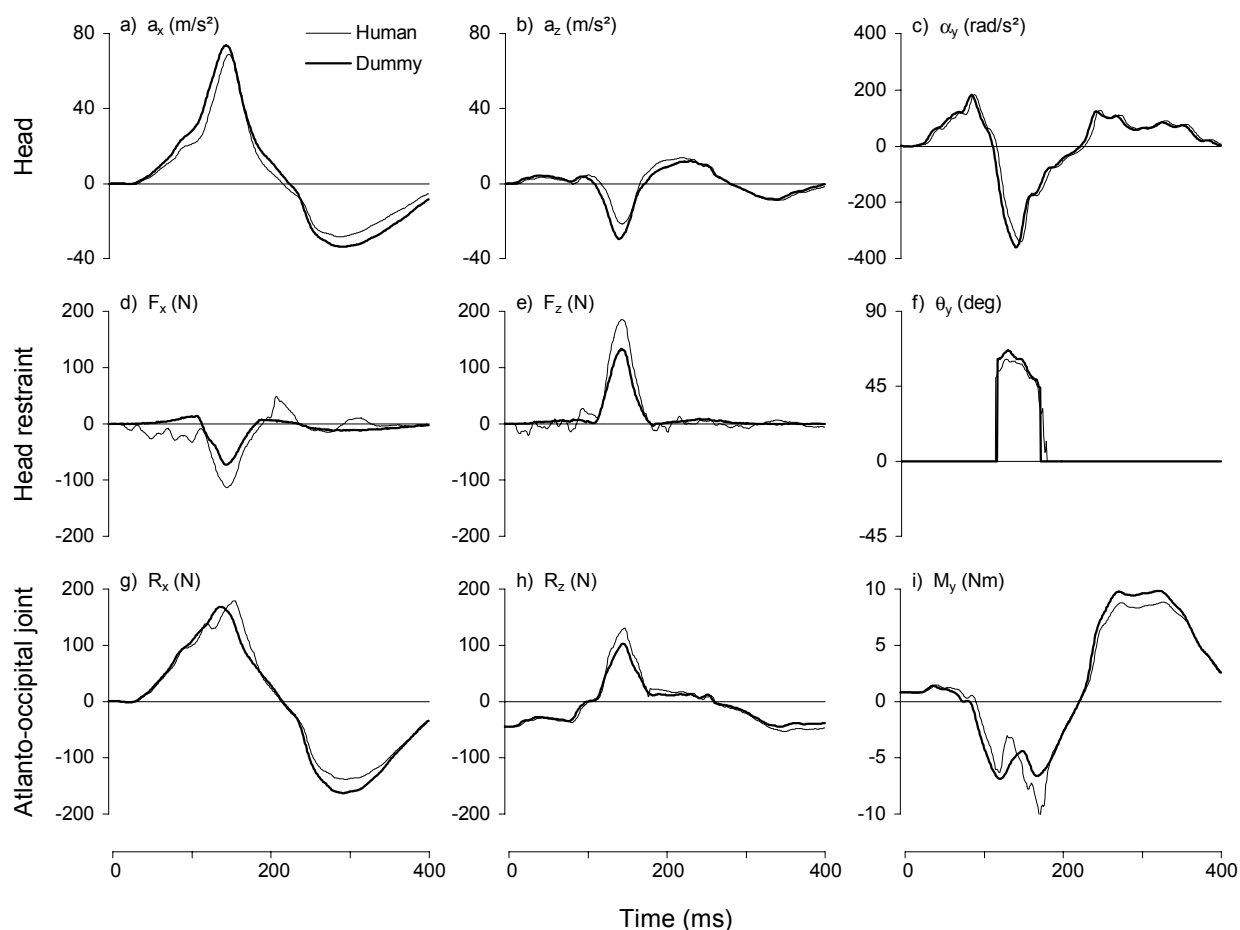


Figure 4. Comparison of the head accelerations (a, b, c), head restraint forces (d, e, f) and atlanto-occipital loads (g, h, i) derived from the externally-mounted transducers (thin line) used for both humans and ATDs and the internally-mounted transducers (thick line) mounted in the ATDs. The test shown was at the 8 km/h level using the Hybrid III.

The absolute angular response at T1 of the Hybrid III did not exhibit the rearward ( $+\theta_y$ ) rotation observed in the human subjects (Figures 5f and 7f). This rearward rotation was observed at T1 in the RID2a, however, the magnitude of the rotation was only about half that observed in the human subjects (Figures 5f and 7f). The Hybrid III did not accurately reproduce the delayed onset, magnitude or rapid direction reversal of either the absolute or relative angular head accelerations (Figures 5i,o and 7i,o). The RID2a captured these responses, although the peak amplitudes were larger at the 4 km/h level (Figures 5i,o) and the rapid direction reversal occurred earlier at the 8 km/h level (Figures 7i,o) than were observed in the human subjects. The magnitude of the absolute head extension angle of the RID2a was similar to the human subjects, but temporally advanced (Figures 5-l and 7-l). Because of its low T1 rotation and early head rotation, the RID2a did not exhibit the initial flexion of the head with respect to T1 observed in the human subjects at both collision severities, however its response in this

regard was better than that of the Hybrid III (Figures 5r and 7r). Absolute head flexion during forward rebound was larger in both ATDs than in the human subjects (Figures 5-l and 7-l, Appendix A).

Head restraint loads for the human subjects had similar horizontal and vertical components at the 4 km/h level (Figures 6a,b). Since head restraint contact did not occur for the Hybrid III at this collision severity, only the small inertial component of the head restraint response was recorded. For the RID2a at the 4 km/h level, the vertical head restraint loads were larger and resulted in a force angle that was about 15 degrees larger than those observed for the human subjects (Figure 6c). At the 8 km/h level, the peak vertical head restraint loads for the human subjects were over twice as large as the peak horizontal loads (Figure 8b). Both this pattern of loading and the absolute magnitude of the head restraint loads were captured by the RID2a, but not the Hybrid III (Figure 8a-c).

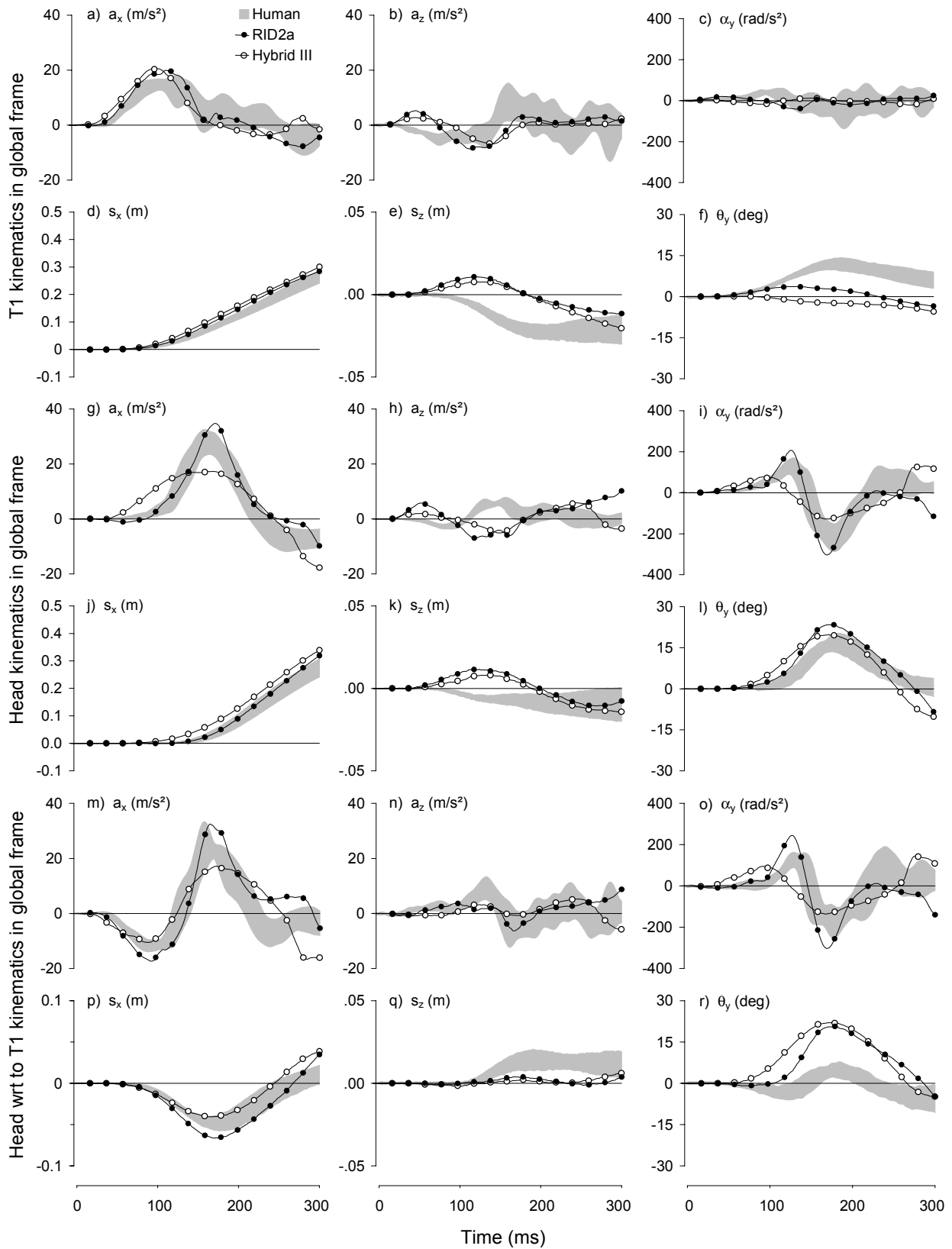


Figure 5. Kinematic responses of T1, head, and head with respect to (wrt) T1 in the global reference frame at a speed change of 4 km/h. Human data shown as shaded corridor ( $\pm 1$  SD); mean response shown for Hybrid III (O) and RID2a (●). a, acceleration; s, displacement;  $\alpha$ , angular acceleration;  $\theta$ , angle; x, y and z subscripts refer to the coordinate axes.

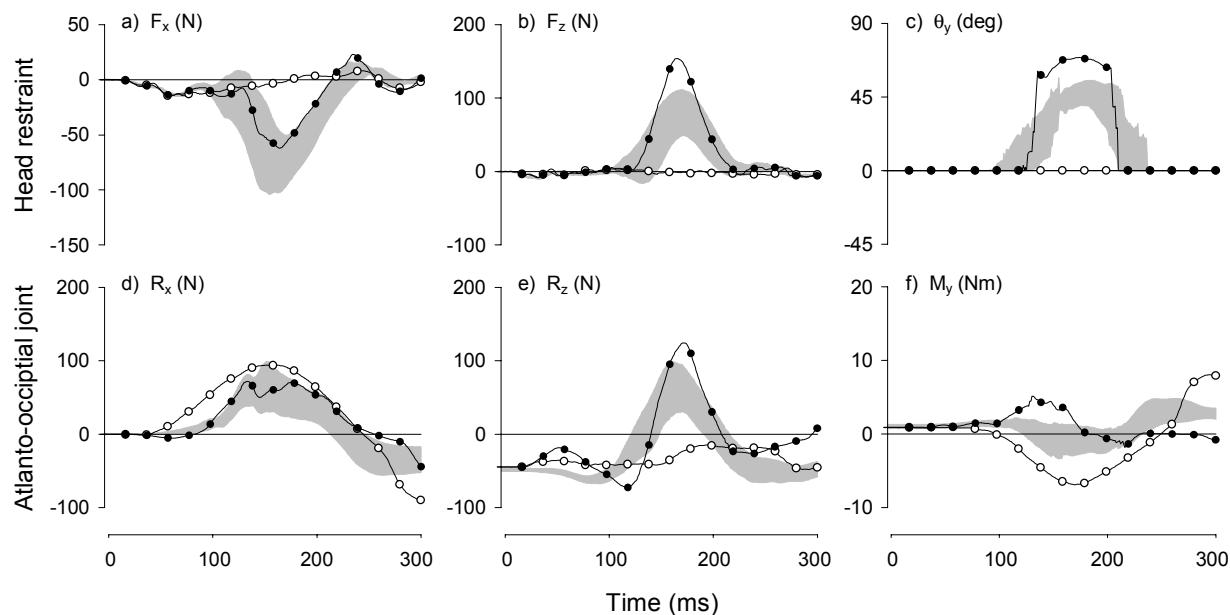


Figure 6. Head restraint loads (a, b) and angle (c), and atlanto-occipital forces (d, e) and moment (f) at a speed change of 4 km/h. Human data shown as shaded corridor ( $\pm 1$  SD); mean response shown for Hybrid III (O) and RID2a (●). The head restraint loads were reported in the global reference frame, whereas the AO joint loads were resolved into the head reference frame. F, head restraint force;  $\theta$ , head restraint force angle; R, AO joint force; M, AO joint moment; x, y and z subscripts refer to the coordinate axes.

The shear and axial loads at the AO joint of the Hybrid III were unaffected by head restraint contact at the 4 km/h level (Figure 6d,e). At the 8 km/h level, head restraint contact did occur for the Hybrid III, however, the early rise in the shear force ( $R_x$  - Figure 8d), the low peak axial force in tension ( $R_z$  - Figure 8e) and the flexor moment applied to the head ( $M_y$  - Figure 8f) were all different than the human subject response. For the RID2a, the shear force ( $R_x$ ) at the AO joint was similar to the human subject data at both collision severities (Figures 6d and 8d). Consistent with the previously-observed vertical kinematics, the axial force ( $R_z$ ) initially diverged from the human subject data. Subsequent interaction with the head restraint produced an exaggerated axial response at the 4 km/h level (Figure 6e), but an appropriate response at the 8 km/h level (Figure 8e). The AO moment was larger in the RID2a than in the human subjects at the 4 km/h level (Figure 6f). At the 8 km/h level, the AO moment in the RID2a was similar to the human response though, like some of its other response parameters, slightly advanced in time (Figure 8f).

Both ATDs produced a graded response in the peak amplitude of most variables between the two collision severities (Table 4). The large gradation in the horizontal head acceleration ( $a_x$ ) and the reversal of the axial force direction at the AO joint in the Hybrid III were related to the absence of head restraint contact at the 4 km/h level and its presence

at the 8 km/h level. The only variable which did not increase in amplitude with increased collision severity was the angular displacement ( $\theta_y$ ) of the head with respect to T1 in the RID2a (Table 4). This value decreased from  $20.8 \pm 1.4$  degrees in the 4 km/h tests to  $16.7 \pm 0.7$  degrees in the 8 km/h tests. Similar absolute head extension angles at both collision severities ( $23.6 \pm 1.5$  deg at 4 km/h;  $24.8 \pm 0.8$  deg at 8 km/h) indicated that this decrease resulted from an increase in the rearward rotation of T1 with collision severity.

## DISCUSSION

The goal of this study was to compare the dynamic response of two anthropomorphic test devices to the dynamic response of near-50<sup>th</sup>-percentile male subjects under otherwise similar test conditions. This study extended the results of earlier ATD validation experiments by comparing both the kinematic and kinetic responses of the head and neck in the presence of head restraint contact.

Prior to head restraint contact, the responses of the human subjects and ATDs were governed largely by seat back interaction, the coupling of the torso and head through the neck, and the head's inertia. The most obvious difference between the responses of the human subjects and ATDs prior to head restraint contact was the vertical motion of both T1 (Figures 5b,e and 7b,e) and the head (Figures 5h,k and 7h,k)

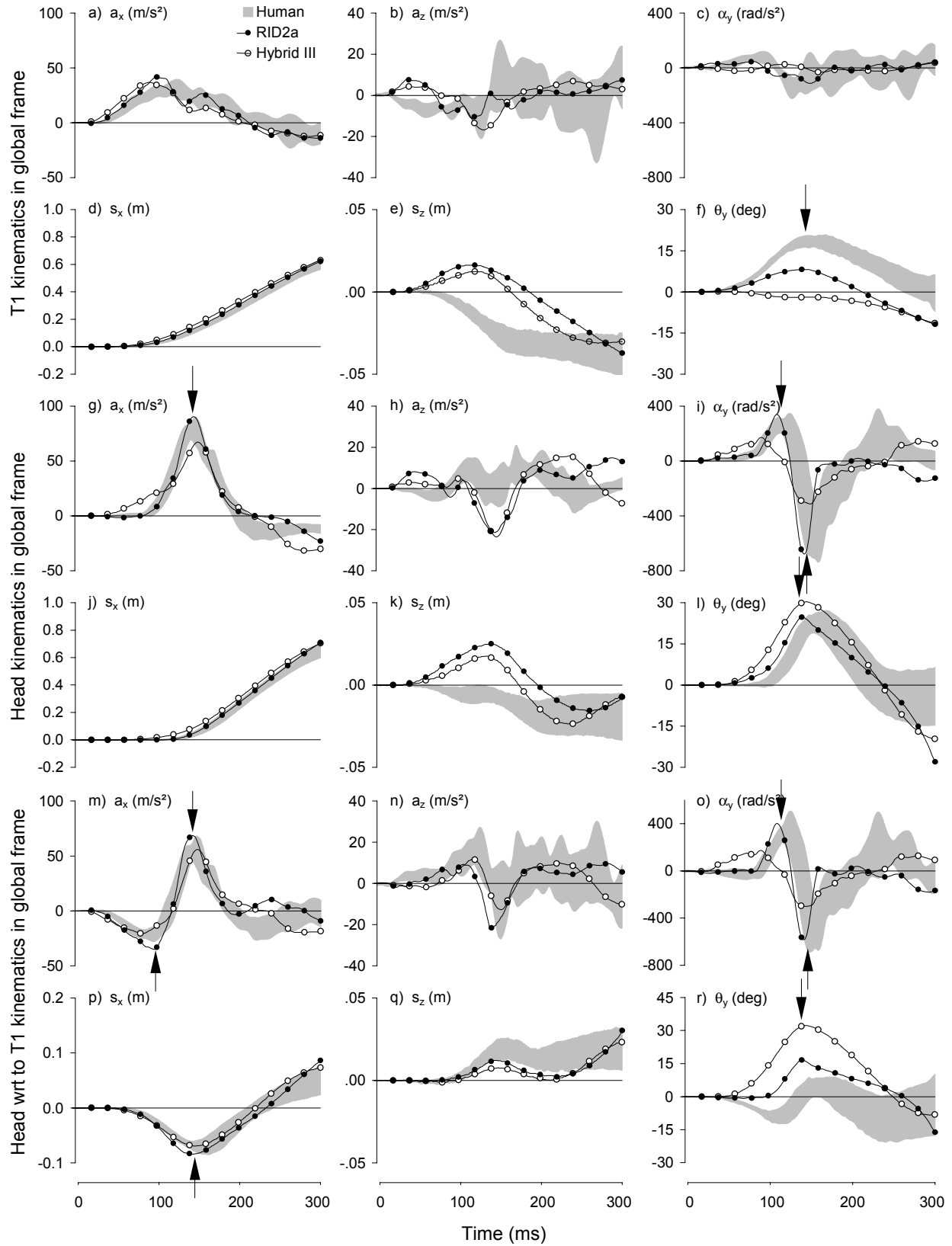


Figure 7. Kinematic responses of T1, head, and head with respect to (wrt) T1 in the global reference frame at a speed change of 8 km/h. Human data shown as shaded corridor ( $\pm 1$  SD); mean response shown for Hybrid III (O) and RID2a (●). Vertical arrows depict the peak responses summarized in Table 3.

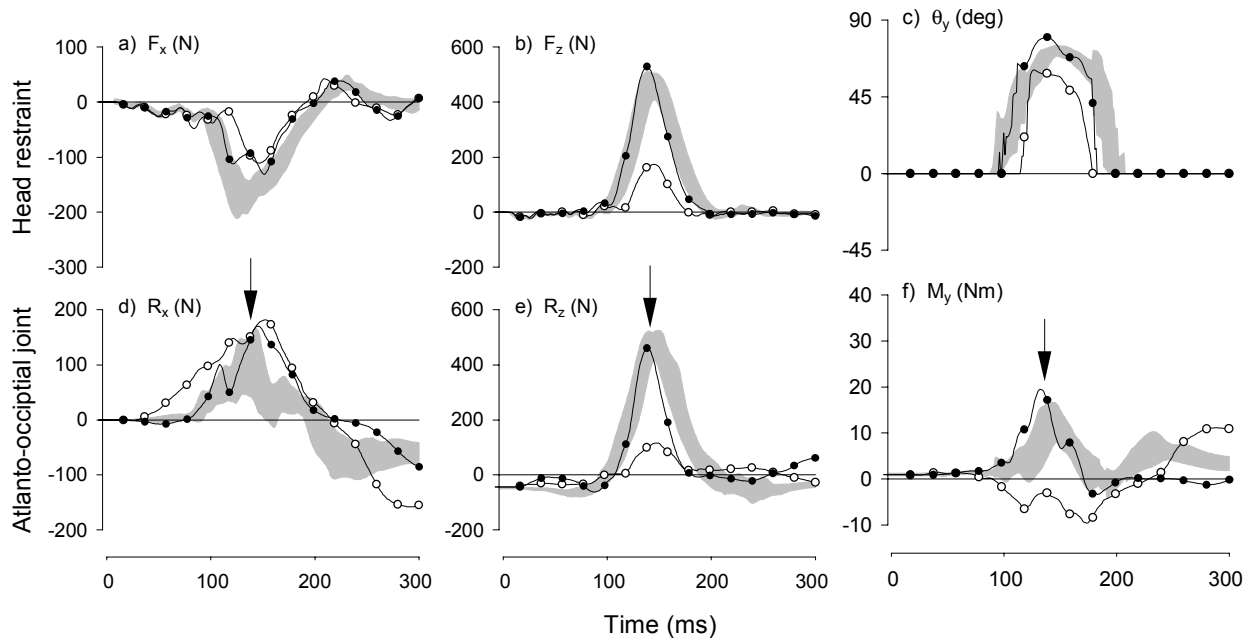


Figure 8. Head restraint loads (a, b) and angle (c), and atlanto-occipital loads (d, e) and moment (f) at a speed change of 8 km/h. Human data shown as shaded corridor ( $\pm 1$  SD); mean response shown for Hybrid III (O) and RID2a (●). The head restraint loads were reported in the global reference frame, whereas the AO joint loads were resolved into the head reference frame. Vertical arrows depict the peak responses summarized in Table 3. F, head restraint force;  $\theta$ , head restraint force angle; R, AO joint force; M, AO joint moment; x, y and z subscripts refer to the coordinate axes.

in the global reference frame. The T1 and head of both ATDs initially accelerated downward (+z), whereas the T1 and head of the human subjects initially accelerated upward (-z). The initial upward acceleration of both T1 and the head has previously been attributed to straightening of the thoracic kyphosis during seat back interaction (Ono et al., 1997) and was reportedly larger when rigid seat backs rather than padded automotive seat backs were used (Davidsson et al., 1999a). The absence of this initial upward acceleration in the ATD responses suggested that neither ATD adequately modeled the initial slouch or degree of thoracic straightening observed in the human subjects. Based on this finding, the RID2a's flexible thoracic element, which was incorporated into the spine to remedy this shortcoming of the Hybrid III, was too stiff to operate effectively for the seat and collision severities used here.

Despite similar initial horizontal T1 accelerations for both ATDs (Figure 5a and 7a), the initial horizontal head acceleration of the Hybrid III rose earlier than both the human subjects and the RID2a (Figures 5g and 7g). A similar early rise was also observed in the angular head acceleration of the Hybrid III (Figures 5i and 7i). These early head kinematics appeared to be caused by an early rise in the horizontal AO joint force ( $R_x$ ) applied to the head of the Hybrid III (Figures 6d and 8d) and implied a more rigid neck in

the Hybrid III than in either the human subjects or the RID2a. The delayed onset of these same parameters in the RID2a was considerably more human-like and likely stemmed from the increased compliance to both horizontal shear and sagittal-plane bending designed into the RID2a neck.

Most of the peak head kinematics and peak AO joint kinetics occurred as a result of head restraint contact, i.e., in the interval between about 100 and 200 ms after bumper contact. Head restraint contact was responsible for the large peak in absolute horizontal head acceleration (Figures 5g and 7g) as well as the rapid reversals and second peaks in the horizontal acceleration of the head relative to T1 (Figures 5m and 7m), the absolute angular head acceleration (Figures 5i and 7i), and the angular acceleration of the head with respect to T1 (Figures 5o and 7o). For each of these parameters, the RID2a produced peak responses that were both larger and more human-like than those of the Hybrid III.

The head restraint loads measured during the human subject tests showed large vertical components (Figures 6b and 8b) and the resultant force applied to the head restraint was angled downward as much as 75 degrees from the global horizontal (Figure 8c). When compensated for the peak absolute head extension angles of about 15 to 25 degrees, the reaction forces applied to the head during head

restraint contact were angled about 50 to 60 degrees upward relative to the head reference frame. These large angles, corroborated in the ATDs by the skull cap load cell, were markedly different from both the purely horizontal forces previously assumed by van den Kroonenberg et al. (1998) in their computation of AO joint loads in human subjects and the resultant force angles of 18 to 25 degrees measured in cadavers by Bertholon et al. (2000). Differences between these studies may be related to the relatively high head restraint position used in the human subject tests conducted by van den Kroonenberg et al. (1998) and the rigid, vertical and high head restraint position

used in the cadaveric tests performed by Bertholon et al. (2000). The head restraint used in the current study was more elliptical in cross section and reached to about the top of the ears in the male subjects used for the current comparisons (Figure 1d). As a result, the back of the head engaged a slightly backward-sloped portion of the head restraint and this angled interaction may have contributed to the large vertical components observed in the head restraint loads.

Differences between the human subjects and ATDs in the initial vertical position of the head with respect to the head restraint appeared to have a relatively small

Table 3. Mean (SD) and coefficient of variation (COV) for selected peak response parameters observed at the 4 km/h level (top of table) and 8 km/h level (bottom of table). Peak responses corresponding to the parameters listed below are highlighted with vertical arrows in Figures 7 and 8.

Parameter	Mean (SD)			COV			
	Human	Hybrid III	RID2a	Human	Hybrid III	RID2a	
$a_x$ (m/s <sup>2</sup> )	30.3 (4.1)	17.5 (0.2)	35.1 (0.5)	13.6	0.9	1.5	
Head $\alpha_{y1}$ (rad/s <sup>2</sup> )	149 (33)	86 (5)	212 (11)	22.3	6.1	5.0	
Head $\alpha_{y2}$ (rad/s <sup>2</sup> )	-267 (48)	-131 (3)	-307 (10)	18.0	2.7	3.2	
$\theta_y$ (deg)	17.8 (3.0)	20.0 (0.6)	23.6 (1.5)	16.8	2.9	6.4	
Tl $\theta_y$ (deg)	12.3 (2.1)	-	3.9 (0.3)	16.9	-	8.5	
$\Delta v = 4$ km/h	Head wrt Tl $a_{x1}$ (m/s <sup>2</sup> )	-12.8 (1.8)	-9.8 (0.3)	-18.9 (1.0)	14.1	3.5	5.4
	Head wrt Tl $a_{x2}$ (m/s <sup>2</sup> )	28.0 (5.8)	17.2 (0.7)	33.8 (1.3)	20.7	3.9	3.8
	Head wrt Tl $s_x$ (m)	-0.050 (0.008)	-0.041 (0.002)	-0.067 (0.002)	15.7	4.8	3.2
	Head $\alpha_{y1}$ (rad/s <sup>2</sup> )	161 (56)	103 (7)	250 (16)	34.8	7.0	6.6
	Head $\alpha_{y2}$ (rad/s <sup>2</sup> )	-229 (57)	-139 (4)	-306 (9)	25.0	2.7	3.0
	$\theta_y$ (deg)	5.93 (2.60)	22.30 (0.55)	20.81 (1.44)	43.8	2.4	6.9
	AO joint $R_x$ (N)	85.2 (29.1)	95.1 (1.6)	74.9 (5.1)	34.1	1.7	6.8
AO joint $R_z$ (N)	77.4 (32.4)	-14.3 (1.3)	126.9 (6.2)	41.9	8.9	4.9	
AO joint $M_y$ (Nm)	3.54 (1.63)	-	5.31 (0.76)	46.1	-	14.3	
$a_x$ (m/s <sup>2</sup> )	82.8 (11.0)	67.5 (1.4)	90.7 (1.2)	13.3	2.1	1.3	
Head $\alpha_{y1}$ (rad/s <sup>2</sup> )	318 (76)	173 (6)	342 (4)	24.0	3.2	1.2	
Head $\alpha_{y2}$ (rad/s <sup>2</sup> )	-732 (174)	-328 (10)	-681 (8)	23.7	3.1	1.2	
$\theta_y$ (deg)	24.6 (4.9)	30.4 (1.3)	24.8 (0.8)	19.9	4.3	3.2	
Tl $\theta_y$ (deg)	19.3 (1.9)	-	12.3 (0.4)	10.0	-	3.1	
$\Delta v = 8$ km/h	Head wrt Tl $a_{x1}$ (m/s <sup>2</sup> )	-25.4 (5.2)	-19.2 (0.6)	-39.1 (1.8)	20.5	3.3	4.6
	Head wrt Tl $a_{x2}$ (m/s <sup>2</sup> )	59.0 (14.6)	53.9 (1.3)	68.2 (2.9)	24.7	2.5	4.3
	Head wrt Tl $s_x$ (m)	-0.073 (0.015)	-0.070 (0.001)	-0.084 (0.003)	20.2	1.9	3.2
	Head $\alpha_{y1}$ (rad/s <sup>2</sup> )	415 (124)	174 (7)	404 (8)	29.8	4.2	2.0
	Head $\alpha_{y2}$ (rad/s <sup>2</sup> )	-681 (153)	-320 (12)	-585 (14)	22.4	3.8	2.4
	$\theta_y$ (deg)	6.42 (5.89)	32.38 (1.05)	16.68 (0.70)	91.7	3.3	4.2
	AO joint $R_x$ (N)	138.8 (47.8)	183.5 (7.2)	171.5 (15.1)	34.4	3.9	8.8
AO joint $R_z$ (N)	503.2 (59.7)	119.6 (8.1)	463.6 (4.6)	11.9	6.8	1.0	
AO joint $M_y$ (Nm)	14.47 (3.96)	-	19.73 (1.33)	27.3	-	6.7	

effect on the head kinematics and neck kinetics. Due to geometric differences in the two ATDs, the initial head height of the RID2a was 4.4 cm above the initial head height of the Hybrid III (Figure 1d). If the height of head contact with the curved forward surface of the head restraint was the chief determinant of the dynamic response, then a similar head restraint force magnitude and a different head restraint force direction would be expected for the two ATDs. The results of the current study, however, showed that a relatively large difference in the peak head restraint force magnitude (RID2a: 538 N; Hybrid III: 206 N) was accompanied by a relatively modest difference in the head restraint force angle (RID2a: 80°; Hybrid III: 61°). This combination of results suggested that differences in the rigidity of head/neck coupling between the two ATDs likely contributed more to the dynamic response during head restraint contact than did differences in initial head height. This interpretation was further supported by the AO joint moment data, which showed that throughout head restraint contact, a flexor moment ( $-M_y$ ) was maintained at the AO joint of the Hybrid III, whereas an extensor moment ( $+M_y$ ) developed at the AO joint of the RID2a (Figure 8f). Although the greater sagittal plane bending stiffness of the Hybrid III neck appeared to provide a better explanation of the differences in the response of the two ATDs, some contribution from the initial differences in head height cannot be ruled out. Further work is need to isolate and quantify the effect of head restraint height on both the head restraint loads and the reaction loads at the AO joint.

The current analysis showed that head restraint contact can have a large effect on the reaction loads at the AO joint. In both the human subjects and the RID2a, head restraint contact produced tensile axial forces at the AO joint that reached 400 to 500 N and an extensor moment applied to the head (flexor moment applied to the neck) of about 12 to 20 Nm during the 8 km/h collision. These were larger than the 250 N force and 10 Nm moment previously reported by Ono et al. (1997) and the 300 to 400 N force and 5 to 10 Nm moment reported by Davidsson et al. (1999a) at speed changes of about 8.6 km/h using standard seats without head restraints. Though different seat backs and protocols were used in these previous studies, the current findings suggested that head restraints may increase neck loading under some conditions.

The neck muscles of the human subjects were relaxed prior to impact. Initially-relaxed neck muscles, rather than initially-tensed neck muscles, were chosen for this study because most individuals with whiplash injury have reported being unprepared for the impact and this unprepared state has been associated with a

Table 4. Gradation of response amplitude with collision severity. Data expressed as response amplitude observed at the 8 km/h level divided by the response amplitude at the 4 km/h level.

Parameter	Response Gradation			
	Human	Hybrid III	RID2a	
$a_x$ (m/s <sup>2</sup> )	2.7	3.9	2.6	
Head $\alpha_{y1}$ (rad/s <sup>2</sup> )	2.1	2.0	1.6	
	$\alpha_{y2}$ (rad/s <sup>2</sup> )	2.7	2.5	2.2
$\theta_y$ (deg)	1.4	1.5	1.1	
T1 $\theta_y$ (deg)	1.6	-	3.1	
$a_{x1}$ (m/s <sup>2</sup> )	2.0	1.9	2.1	
$a_{x2}$ (m/s <sup>2</sup> )	2.1	3.1	2.0	
Head wrt T1 $s_x$ (m)	1.5	1.7	1.3	
$\alpha_{y1}$ (rad/s <sup>2</sup> )	2.6	1.7	1.6	
$\alpha_{y2}$ (rad/s <sup>2</sup> )	3.0	2.3	1.9	
$\theta_y$ (deg)	1.1	1.5	0.8	
AO joint	$R_x$ (N)	1.6	1.9	2.3
	$R_z$ (N)	6.5	-8.4	3.7
	$M_y$ (Nm)	4.1	-	3.7

greater incidence of long-term symptoms (Sturzenegger et al., 1994). The kinematics and kinetics of initially-relaxed subjects should therefore be of more interest to whiplash ATD designers. The collisions evoked a reflexive neck muscle activation in the human subjects about 80 to 100 ms after impact (see Brault et al., 2000 for a detailed analysis of the neck muscle response). This muscle activation likely altered the rotational stiffness of the human head/neck system in the sagittal plane during the dynamic response and potentially explained the smaller head flexion in the human subjects during forward rebound than observed in either ATD (Appendix A).

Although a muscle analog was not present in either ATD, the small amount of rotational play about the mediolateral axis at the AO joint of the RID2a appeared to capture the transition from a relatively flexible head/neck connection, consistent with relaxed neck muscles, to a stiffer connection, consistent with active neck muscles. Whereas the initial horizontal head acceleration, angular head acceleration, AO shear force and AO moment of the Hybrid III all showed evidence of a rigid link between the torso and neck, these same parameters in the RID2a demonstrated an initial loose coupling observed in initially-relaxed human subjects. Further work is needed to assess which ATD better models the response of aware subjects who have tensed their neck muscles prior to impact.

Both ATDs exhibited a positive gradation in the magnitude of their dynamic response variables with collision severity. Only one variable, the rotation of the head with respect to T1 in the RID2a did not exhibit this pattern. The decreased relative head rotation in the RID2a at the 8 km/h level was the result of similar absolute head rotations at both speed changes combined with a larger absolute T1 rotation at the 8 km/h level. As discussed earlier, increased flexibility of the thoracic spine may improve this response.

It is currently not possible to conclude whether either ATD is sufficiently valid to be a useful tool in the study or prevention of whiplash injury because the specific kinematics and kinetics which cause whiplash injury are not known with certainty. Current proposed mechanisms of whiplash injury include dorsal root ganglion injury (Örtengren et al., 1996; Svensson et al., 1993), capsular ligament impingement (Kaneoka et al., 1999) and facet joint capsular ligament strain (Winkelstein et al., 2000; Siegmund et al., 2001). These mechanisms rely on either rapid relative horizontal acceleration between the superior and inferior ends of the cervical spine or combined bending and shear in the neck. If these specific kinematic and kinetic parameters are used as a criterion for ATD validity, then the RID2a is a better tool with which to design seating systems to minimize the potential for whiplash injury than is the Hybrid III. The differences between the Hybrid III and human subject responses were consistent with a neck and torso that were too stiff - a conclusion that have been previously reached by other researchers (Scott et al., 1993; Geigl et al., 1995; Davidsson et al., 1999a, 1999b; Gotou et al., 1999; Cappon et al., 2000).

Many variables other than collision severity may influence occupant response and the potential for whiplash injury. For instance, the peak response amplitudes in human subjects have previously been shown to vary with both head restraint backset and height (Siegmund et al., 1999). Based on the earlier comparison of head restraint loads between this and previous studies, the shape of the head restraint may also be an important factor. A limitation of the current study is the use of only one seat and one head restraint position. If whiplash ATDs are to be used to evaluate seat and head restraint designs, then the gradation of their responses to these other variables also needs to be validated against the human subject response.

## CONCLUSIONS

The results of the current study indicated that the prototype of the new RID2 whiplash ATD produced horizontal and angular responses at the head and AO

joint that were more human-like than the Hybrid III. The absolute vertical kinematics at both T1 and the head were different than those observed in the human subjects, however the relative vertical kinematics and the vertical AO joint loads were similar. The head restraint loads observed in both the human subjects and the ATDs had larger vertical components than previously reported and suggested that subtle features of the head restraint shape and position may affect the magnitude of the loads in the neck during a low-speed rear-end collision.

## ACKNOWLEDGMENTS

The authors wish to acknowledge Mr. Eric Stanley and Mr. Gordon Morgan of First Technology Safety Systems, Plymouth, MI for the use of the Hybrid III ATD and instrumentation; and Mr. Jeff Nickel of MacInnis Engineering Associates for his assistance in conducting the experiments.

## REFERENCES

- Bertholon, N., Robin, S., Le-Coz, J.-Y., Potier, P., Lassau, J.-P., and Skalli, W. (2000). Human head and cervical spine behaviour during low-speed rear-end impacts: PMHS sled tests with a rigid seat. Proc. 2000 International IRCOBI Conference on the Biomechanics of Impact, pp. 265-277. IRCOBI Secretariat, Bron, France.
- Brault, J.B., Siegmund, G.P., and Wheeler, J.B. (2000). Cervical muscle response during whiplash: Evidence of a lengthening muscle contraction. *Clinical Biomechanics* 15: 426-435.
- Cappon, H.J., Philippens, M.M.G.M., van Ratingen, M.R., and Wismans, J.S.H.M. (2000). Evaluation of dummy behavior during low severity rear impact. Proc. 2000 International IRCOBI Conference on the Biomechanics of Impact, pp. 53-66. IRCOBI Secretariat, Bron, France.
- Davidsson, J. (1999). BioRID II final report. Crash Safety Division, Department of Machine and Vehicle Design, Chalmers University of Technology, Göteborg, Sweden.
- Davidsson, J. (2000). Development of a mechanical model for rear impacts: Evaluation of volunteers responses and validation of the model. PhD Thesis, Chalmers University of Technology, Göteborg, Sweden.
- Davidsson, J., Lövsund, P., Ono, K., Svensson, M.Y., and Inami, S. (1999a). A Comparison between volunteer, BioRID P3 and Hybrid III performance in rear impacts. Proc. 1999 International IRCOBI

- Conference on the Biomechanics of Impact, pp. 165-178. IRCOBI Secretariat, Bron, France.
- Davidsson, J., Flogård, A., Lövsund, P., and Svensson, M.Y. (1999b). BioRID P3 - Design and performance compared to Hybrid III and volunteers in rear impacts at  $\Delta V=7$  km/h (99SC16). Proc. 43<sup>rd</sup> Stapp Car Crash Conference, pp. 253-265. Society of Automotive Engineers, Warrendale, PA.
- Diffrient, N., Tilley, A.R., and Bardagiy, J.C. (1974). *Humanscale Manual*. The MIT Press, Cambridge, MA.
- Geigl, B.C., Steffan, H., Dippel, Ch., Muser, M.H., Walz, F., and Svensson, M.Y. (1995). Comparison of head-neck kinematics during rear end impact between standard Hybrid III, RID neck, volunteers and PMTO's. Proc. 1995 International IRCOBI Conference on the Biomechanics of Impact, pp. 261-270. IRCOBI Secretariat, Bron, France.
- Gotou, T., Ono, K., Inami, S., Kaneoka, K., and Davidsson, J. (1999). A comparison between human volunteer and three types of dummies head/neck/torso response in rear-end sled impacts (9939974). Proc. 1999 Spring Convention of Japan Society of Automotive Engineering, 75-99, pp. 17-20.
- Hubbard, R., and McLeod, D. (1974). Definitions and development of a crash dummy head (741193). In *Hybrid III: The First Human-Like Crash Test Dummy (PT-44)*, ed. S.H. Backaitis and H.J. Mertz, pp. 95-110. Society of Automotive Engineers, Warrendale, PA.
- Kaneoka, K., Ono, K., Inami, S., and Hayashi, K. (1999). Motion analysis of cervical vertebrae during whiplash loading. *Spine* 24: 763-770.
- Lawrence, J.M., Siegmund, G.P., and Nickel, J.S. (1997). Measuring head restraint force and point of application during low-speed rear-end automobile collisions (970397). In *Occupant Protection and Injury Assessment in the Automotive Crash Environment (SP-1231)*, ed. A. Irwin and S. Backaitis, pp. 225-37. Society of Automotive Engineers, Warrendale, PA.
- Mertz, H.J., and Patrick, L.M. (1967). Investigations of the kinematics and kinetics of whiplash (670919). Proc. 11th Stapp Car Crash Conference, pp. 267-317. Society of Automotive Engineers, Warrendale, PA.
- Najjar, M.F., and Rowland, M. (1987). *Anthropometric Reference Data and Prevalence of Overweight, United States, 1976-80, Data from the National Health Survey series 11, No. 238 (PHS) 87-1688*. National Center for Health Statistics, Department of Health and Human Services, Hyattsville, MD.
- Ono, K., Kaneoka, K., Wittek, A., and Kajzer, J. (1997). Cervical injury mechanism based on the analysis of human cervical vertebral motion and head-neck-torso kinematics during low speed rear impact (973340). Proc. 41st Stapp Car Crash Conference, pp. 339-356. Society of Automotive Engineers, Warrendale, PA.
- Örtengren, T., Hansson, H.-A., Lövsund, P., Svensson, M.Y., Suneson, A., and Säljö, A. (1996). Membrane leakage in spinal ganglion nerve cells induced by experimental whiplash extension motion: A study in pigs. *Journal of Neurotrauma* 13: 171-180.
- Padgaokar, A.J., Krieger, K.W., and King, A.I. (1975). Measurement of angular acceleration of a rigid body using linear accelerometers (No. 75-APMB-3). *Transactions of the American Society of Mechanical Engineers*, pp. 522-526.
- Queisser, F., Bluthner, R., and Seidel, H. (1994). Control of positioning the cervical spine and its application to measuring extensor strength. *Clinical Biomechanics* 9: 157-161.
- Scott, M.W., McConnell, W.E., Guzman, H.M., et al. (1993). Comparison of human and ATD head kinematics during low-speed rearend impacts (930094). In *Human surrogates: Design, development and side impact protection (SP-945)*, pp. 1-8. Society of Automotive Engineers, Warrendale, PA.
- Severy, D.M., Mathewson, J.H., and Bechtol, C.O. (1955). Controlled automobile rear-end collisions, An investigation of related engineering and medical phenomena. *Canadian Services Medical Journal* 11: 727-759.
- Siegmund, G.P. (2001). *The reflex response of human neck muscles to whiplash-like perturbations*. PhD Thesis, University of British Columbia, Vancouver, BC, Canada.
- Siegmund, G.P., King, D.J., Lawrence, J.M., Wheeler, J.B., Brault, J.R., and Smith, T.A. (1997). Head/neck kinematic response of human subjects in low-speed rear-end collisions (973341). Proc. 41st Stapp Car Crash Conference, pp. 357-385. Society of Automotive Engineers, Warrendale, PA.

- Siegmund, G.P., Heinrichs, B.E., and Wheeler, J.B. (1999). The influence of head restraint and occupant factors on peak head/neck kinematics in low-speed rear-end collisions. *Accident Analysis and Prevention* 31: 393-407.
- Siegmund, G.P., Myers, B.S., Davis, M.B., Bohnet, H.F., and Winkelstein, B.A. (2001). Mechanical evidence of cervical facet capsule injury during whiplash. A cadaveric study using combined shear, compression, and extension loading. *Spine* 26(19): 2095-2101
- Society of Automotive Engineers (1989). SAE recommended practice: Instrumentation for impact tests (SAE J211 Jun 88). 1989 SAE Handbook, Volume 4, On-highway vehicles and off-highway machinery, pp. 34.184 - 34.191. Society of Automotive Engineers, Warrendale, PA.
- Sturzenegger, M., DiStefano, G., Radanov, B.P., and Schnidrig, A. (1994). Presenting symptoms and signs after whiplash injury: The influence of accident mechanisms. *Neurology* 44: 688-693.
- Svensson, M.Y., Aldman, B., Lövsund, P., Hansson, H.A., Seeman, T., Suneson, A., and Örtengren, T. (1993). Pressure effects in the spinal canal during whiplash extension motion – A possible cause of injury in the cervical spinal ganglia. *Proc. 1993 International IRCOBI Conference on the Biomechanics of Impact*, pp. 189-200. IRCOBI Secretariat, Bron, France.
- Svensson, M.Y., and Lövsund, P. (1992). A dummy for rear-end collisions – Development and validation of a new dummy-neck. *Proc. 1992 International IRCOBI Conference on the Biomechanics of Impact*, pp. 299-310. IRCOBI Secretariat, Bron, France.
- Thunnissen, J.G.M., van Ratingen, M.R., Beusenberg, M.C., and Janssen, E.G. (1996). A dummy neck for low severity impacts (96-S10-O-12). *Proc. 15<sup>th</sup> International Technical Conference on Enhanced Safety of Vehicles*, pp.1665-1678. National Highway Traffic Safety Administration, Washington, DC.
- van den Kroonenberg, A., Philippens, M., Cappon, H., Wismans, J., Hell, W., and Langwieder, K. (1998). Human head-neck response during low-speed rear end impacts. *Proc. 42<sup>nd</sup> Stapp Car Crash Conference*, pp. 207-221. Society of Automotive Engineers, Warrendale, PA.
- Winkelstein, B.A., Nightingale, R.W., Richardson, W.J., and Myers, B.S. (2000). The cervical facet capsule and its role in whiplash injury: A biomechanical investigation. *Spine* 25: 1238-1246.

## APPENDIX - HIGH SPEED VIDEO SEQUENCES

